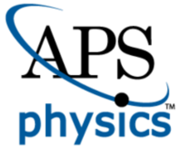

CHORUS

This is the accepted manuscript made available via CHORUS. The article has been published as:

Effect of oxygen gas pressure on the kinetics of alumina film growth during the oxidation of Al(111) at room temperature

Na Cai, Guangwen Zhou, Kathrin Müller, and David E. Starr

Phys. Rev. B **84**, 125445 — Published 29 September 2011

DOI: 10.1103/PhysRevB.84.125445

Effect of oxygen gas pressure on the kinetics of alumina film growth during the oxidation of Al(111) at room temperature

Na Cai, Guangwen Zhou*

Department of Mechanical Engineering & Multidisciplinary Program in Materials Science and Engineering, State University of New York, Binghamton, NY 13902

Kathrin Müller, David E. Starr

Center for Functional Nanomaterials, Brookhaven National Laboratory, Upton, NY 11973

Abstract

We have studied the effect of oxygen pressure on the self-limiting oxidation of an Al(111) surface at room temperature for oxygen pressures from 1×10^{-8} to 5 Torr. Using x-ray photoelectron spectroscopy measurements we monitor the oxidation kinetics and the oxide film thickness for different oxidation times and pressures. After a rapid initial growth stage, the oxide film reaches a saturated thickness, which depends on the oxygen pressure. The kinetic potential, oxide growth rate, oxide film limiting thickness, and the density of oxygen anions on the oxide surface are determined by the measured oxidation kinetics. These quantities show a Langmuir isotherm dependence on the oxygen gas pressure.

* To whom all correspondence should be addressed. E-mail: gzhou@binghamton.edu

1. Introduction

The oxidation of metal surfaces is of great importance for a wide range of technological applications including gate oxides, electrochemistry, corrosion, lubrication, and heterogeneous catalysis. Aluminum oxide is a good gate insulator for thin film transistor (TFT) applications. For example a double-layered Al_2O_3 gate insulator can improve the bias stability of ZnO TFTs [1]. The shrinking of SiO_2-based gate dielectrics in microelectronics reduces dielectric reliability and significantly increases leakage current. Aluminum oxide due to its high dielectric constant (Al_2O_3 ~9) [2] and wide band gap (9 eV) [3] is a promising candidate for gate oxide material. Even though the Al_2O_3-SiO_2 compound dielectric constant is lower compared to alumina itself, it has emerged as one of the promising high-κ dielectric candidates [4]. Due to its chemical and thermal stability, aluminum oxide is also a good corrosion inhibitor and thermal barrier. An example is the improvement of the durability of Si-based ceramics as a protective coating [5]. Moreover, thin film aluminum oxide surfaces have recently received much attention as supports for metal clusters which serve as model systems for understanding heterogeneous catalytic processes [6].

Amorphous aluminum oxide films formed by low-temperature oxidation of aluminum fulfill the unique functions for these applications in part due to negligible growth strain, no grain-boundaries, and large bond-flexibility at the oxide-metal interface. The distinction between low-temperature and high-temperature oxidation is that low-temperature oxidation relies on an electrochemical mechanism as opposed to thermal activation for high temperature oxidation [7]. In general, the oxidation of Al starts with the dissociative chemisorption of O_2 from the gas phase via a charge transfer from the metal to the oxygen. To grow more than one oxide layer, Al ions must cross the growing oxide film to reach the surface. At low-temperatures, oxidation via thermally activated diffusion is negligibly small and ionic diffusion through the oxide film is driven by the electric field established by tunneling electrons across

the oxide film due to the potential difference (called the Mott Potential) of the metal-oxide work function and the oxygen-oxide work function. Since the rate of electron transport across the oxide film by tunneling decreases exponentially with increasing oxide film thickness, the requirement for charge neutrality of coupled currents of electrons and cations implies there is a limiting oxide film thickness at low temperatures [8, 9].

The amorphous alumina films formed by low-temperature oxidation can be well described locally by a close packing of oxygen anions with the Al cations distributed over the octahedral and tetrahedral interstices [10]. The alumina films formed at low temperature exhibit a deficiency of Al cations (as compared to γ-Al_2O_3) [11-13]. Therefore, it is expected that the oxide film growth is limited by ionic migration of cations under the influence of the electric field $E = -V_M/L(t)$ due to the Mott potential V_M and, as a result, the oxide film growth rate follows [14, 15]

$$\frac{dL}{dt} = \Omega n \nu \exp\left(\frac{-U + qaV_M / L}{kT}\right), \tag{1}$$

where L denotes the oxide film thickness at time t, Ω is the volume of oxide formed per transported cation, n is the number of cations per unit area which may jump through the diffusion barrier U, q is the charge of the migrating ions, 2a is the distance between two adjacent potential minima, ν is the attempt frequency for ion migration, k is the Boltzmann constant and T the temperature. By defining the effective limiting thickness of the oxide film L_{lim} as the thickness reached when $dL/dt \leq 10^{-5}$ Å/s (this corresponds to an oxide-film growth rate of less than one 'oxide' monolayer per 10^5 s and the oxide film thickness can be considered constant on laboratory time scales), integration of eq. (1), yields an inverse logarithmic growth law of the oxide film with L_{lim} given by [15]

$$\frac{1}{L_{\mathrm{lim}}} = -\frac{k \ln\left(10^{-15} / \Omega n \nu\right)}{qaV_M} T - \frac{U}{qaV_M}. \tag{2}$$

As indicated in eq. (2), this limiting thickness should depend linearly on the oxidation temperature. Extensive studies have focused predominantly on how the oxide film growth kinetics and limiting thickness can be manipulated by the oxidation temperature without much consideration of the effect of oxygen pressure [10]. It is generally believed that the magnitude of the Mott potential is determined by the potential difference of the metal-oxide work function Φ_m and the oxygen-oxide work function Φ_o, i.e., $V_M = (\Phi_m-\Phi_o)/e$, where e is the elementary charge of electron. Since the work function is an intrinsic property, a tacit assumption made in the Cabrera-Mott oxidation model is that the Mott potential V_M is constant during oxide film growth for a particular metal-oxide system. However, our recent work [16] revealed that the actual value of the self-generated electrostatic potential (designated as the kinetic potential V_K) [17, 18] is oxygen pressure dependent and can be much smaller than the Mott potential, V_M. As a result, the limiting thickness of the oxide film shows a strong dependence on the oxygen pressure although the limiting thickness as defined in eqs. (1 and 2) does not contain any explicit pressure dependence. In this work we extend our previous study [16] by examining the effect of oxygen pressure on the oxidation kinetics including the average oxidation rates, the limiting thickness of the oxide film, and number density of oxygen anions on the oxide surface as well as the kinetic potential. Our results reveal that since these kinetic quantities are proportional to the number density of oxygen anions on the oxide surface they all display a Langmuir isotherm-like dependence on the oxygen gas pressure.

2. Experimental

The experiments were carried out in an ultrahigh vacuum chamber equipped with an x-ray photoelectron spectrometer – SPECS Phoibos 100 MCD analyzer, low-energy electron diffraction (LEED)

and an Ar^+ ion sputtering gun. The chamber typically has a base pressure of 2×10^{-10} Torr. A non-monochromatized Al-Kα X-ray source was used for the x-ray photoelectron spectroscopy (XPS) studies. The Al (111) single crystal is a 'top-hat' disk (1 mm thick and 8 mm in diameter), purchased from Princeton scientific Corp., cut to within 0.1° to the (111) crystallographic orientation and polished to a mirror finish. The sample was heated via a ceramic button heater and its temperature monitored with a type-K thermocouple. The crystal was cleaned by cycles of Ar^+ sputtering at 300 K (1×10^{-5} Torr of Ar^+, 1 μA cm^{-2}, 1.0 keV) followed by annealing at 700 K. The surface cleanliness was checked with XPS.

Oxygen gas (purity = 99.9999%) was introduced to the system through a variable pressure leak valve and the sample was oxidized at room temperature (300 K) under a controlled oxygen pressure, p(O2). Following oxidation at each oxygen pressure, the sample was cleaned until no oxygen was detected by XPS. For the initial stages of oxidation (oxygen coverages much less than 1 monolayer where no attenuation of the Al(2p) metallic peak was detectable), the oxide film thickness was estimated with XPS by calculating the ratio of integrated O 1s and Al 2p core level peak intensities with atomic sensitivity factors (ASF) [19] that are correlated with the Al_2O_3 monolayer thickness (1 Al_2O_3 ML ~ 0.2nm) [20]. For thicker, continuous oxide films formed at higher oxygen gas exposures (including longer time oxygen exposure at 1×10^{-8} Torr and all pressures above 1×10^{-8}) thicknesses are estimated from the attenuation of the metallic Al(2p) XPS peak in the oxide films with the photoelectron attenuation length for Al_2O_3 (λ = 16.7± 0.6Å) [21, 22] by using the formula $d = -\lambda \cos\theta \ln\left(\frac{A}{A_0}\right)$, where A is the area of Al metallic peak after oxygen exposure, A_0 is the area of the Al metallic peak before oxygen exposure, λ is the inelastic mean free path and θ is the detection angle relative to the surface normal, 0° in our geometry.

3. Results

We oxidized a clean Al(111) crystal with oxygen gas at various pressures from 1×10^{-8} to 5 Torr. For each oxygen pressure, a limiting oxide film thickness is reached after long time exposure. XPS measurements are performed with the Al(111) surface being exposed to different oxygen pressures for different time periods. Fig. 1 shows representative XPS spectra of the Al 2p core level peaks obtained from the Al surface oxidized to the limiting thickness for different oxygen pressures. The position of the metallic Al (2p) peak for different oxygen exposures is nearly constant at 72.8 eV while its intensity decreases with increasing oxygen pressure. On the other hand, another peak - oxidic Al (2p) peak at a larger binding energy becomes visible and increases in intensity with increasing oxygen gas pressure, suggesting a strong dependence of the limiting thickness of the oxide film on the oxygen pressure.

Fig. 2 shows kinetic growth curves measured with XPS over a time period extending to approximately 5 hrs for each oxygen pressure. The oxygen gas exposure was interrupted for the XPS measurements. From the series of oxygen uptake curves at different oxygen pressures, a correlation between the oxidation kinetics and oxygen pressure was obtained. For each oxygen pressure, we observe an initial rapid increase of the oxide thickness, followed by a drastic reduction of the oxide film growth at longer times. Extrapolating the time dependences in Fig. 2 to about 250 min, we derive the effective limiting oxide-film thickness as the value of the thickness reached when the oxide film growth rate is less than 10^{-5} Å/s (i.e., less than one 'oxide' ML per 10^{5} s). As shown in Fig. 3, these limiting thicknesses increase with increasing oxygen gas pressure.

The average oxide film growth rate for the different oxygen pressures is also determined from the oxidation kinetic measurements. The average oxide growth rate is estimated as the effective limiting oxide-film thickness divided by the time it takes to reach the effective limiting thickness. Fig. 4 shows the

obtained oxide growth rates at the different oxygen pressures. A clear trend can be noted: the oxide film growth rate increases with increasing oxygen pressure.

In order to compare the stoichiometry of the oxide films with that of bulk material, the ratio of the integrated oxidic Al core level peak area to the integrated oxygen core level peak area is used to estimate the stoichiometric composition of Al and O in the oxide films. An absolute stoichiometric composition for each film can be calculated by using a reference XPS spectrum. Here the experimental XPS spectra of a well-defined oxide thin film formed by oxidizing NiAl(110) (O : Al = 13 : 10) [23] from our system is used. The obtained O/Al peak intensity ratios of the oxide films formed with the different oxygen pressures are relatively constant, which gives a stoichiometry of $Al_{2-x}O_3$ where x=0.24. By comparing to γ-Al_2O_3 (O : Al = 3 : 2), it confirms that the oxide films are Al cation deficient, for which the outward diffusion of Al cations is favored over the inward diffusion of oxygen anions for oxide film growth [15].

The kinetic potential V_K is also evaluated using the coefficients determined by fitting the experimental data shown in Fig. 2 to Eq. 2. The value of the kinetic potential for each oxygen pressure is given in Fig. 5. Fig. 5 shows that the kinetic potential V_K increases with increasing oxygen gas pressure. By comparing the oxidation kinetics of a freshly cleaned Al(111) surface with that of an Al(111) surface oxidized by step-wise increases in oxygen pressure, we note that both give similar limiting-thicknesses of the oxide films and kinetic potentials at the same oxygen gas pressure, irrespective of whether oxidation occurs on a surface covered with a pre-existing oxide layer formed at a lower oxygen pressure or the surface is clean Al without a pre-existing oxide film [16].

Due to the separation of the adsorbed oxygen ions on the surface from Al cations at the metal-oxide interface by the oxide film, a parallel plate capacitor is formed with a potential difference given by the kinetic potential V_K. Based on the capacitor-like model, the density of chemisorbed oxygen anions on

the oxide film surface, can be calculated via $N = \frac{V_K \varepsilon_0 \kappa}{L_{\lim} e}$ where N is the number density of chemisorbed oxygen anions on the oxide surface, ε_0 is electric constant in vacuum, κ is the relative permittivity and can be taken equal to κ= 9.6 and L_{lim} is the limiting thickness as given in Fig. 3. Our results indicate that the maximum density of oxygen anions on the oxide surface is reached for oxygen pressures of ~ 1 Torr, resulting in the maximum oxide film limiting thickness for room-temperature oxidation. For further oxygen gas pressure increases to 5 Torr, no more oxygen uptake is observed. Fig. 6 shows the obtained number density of the chemisorbed oxygen ions on the oxide surface for the different oxygen pressures. It should be noted that the number density of chemisorbed oxygen anions increases with the oxygen pressure and saturates at pressures approximately > 1 Torr.

4. Discussion

We have observed a strong dependence of the limiting oxide film thickness on the oxygen gas pressure, which is in contrast to the behavior expected for cation-diffusion-controlled oxide film growth under the assumption of a constant Mott potential for a particular metal-oxide system. The theoretical fitting of our experimental data to the self-limiting oxide growth of the Cabrera-Mott model leads to the determination of the kinetic potential V_K, which is found to bear a strong dependence on the oxygen gas pressure. In addition, the average oxide growth rate as well as the density of oxygen anions on the oxide surface is also found to show a similar dependence on the oxygen gas pressure.

As shown in Fig. 6, the effective charge, resulting from adsorbed oxygen anions present on the oxide surface, is much smaller than the value expected for a stoichiometric Al_2O_3 , suggesting that the oxygen surface coverage is less than the saturation level at low oxygen gas pressures (< ~ 1 Torr).

According to the Langmuir isotherm for dissociative gas adsorption, the dependence of the equilibrium oxygen anion coverage on the oxygen gas pressure $p(O_2)$ is given by $\Theta = \frac{\sqrt{b\mathbf{p}(\mathbf{O}_2)}}{1+\sqrt{b\mathbf{p}(\mathbf{O}_2)}}$, where b is a constant which depends on temperature only [24]. The solid line in Fig. 6 is the fit to the data points based on the Langmuir isotherm and their agreement reflects the fact that the surface coverage of oxygen anions is well-described by equilibrium dissociative adsorption of oxygen molecules at the various oxygen pressures. Since the kinetic potential originates from the adsorbed oxygen anions on the oxide surface and their Al cation counterparts at the metal-oxide interface, it is reasonable to expect a linear dependence of the kinetic potential V_K on the amount of adsorbed oxygen that can be ionized by tunneling electrons. That is,

$$V_K = C\frac{\sqrt{b\mathbf{p}(\mathbf{O}_2)}}{1+\sqrt{b\mathbf{p}(\mathbf{O}_2)}}, \tag{3}$$

where C is a constant coefficient. The solid line in Fig. 5 corresponds to a fit to the kinetic potential calculated from our experimental data to Eq. (3). A similar dependence of the oxide film limiting thickness on the oxygen pressure can be derived by inserting the above V_K into Eq. (2) and its fit to the limiting thickness is given by the solid line in Fig. 3.

Fig. 4 reveals that the average oxide growth rate increases with increasing the oxide pressure. By combining the equations of 2 and 3, the average oxide film growth rate, R, can be determined as follows

$$R = \frac{L_{\lim}}{\Delta t} = -\left[\frac{qa/\Delta t}{kT\ln\left(10^{-15}/\Omega n\nu\right)+U}\right]\left(\frac{C\sqrt{b\mathbf{p}(\mathbf{O}_2)}}{1+\sqrt{b\mathbf{p}(\mathbf{O}_2)}}\right), \tag{4}$$

In Eq. 4, Δt is the oxidation time required to reach the limiting thickness. As can be seen from Fig. 2, a similar oxidation time Δt is needed to reach the limiting thickness of the oxide films at the different

oxygen pressures. Since the oxide film formed at a higher oxygen pressure has a larger limiting thickness, the oxide film has a faster initial growth rate. The fitting to the average oxide film growth rates by Eq. (4) is given by the solid line in Fig. 4 and a good agreement is noted. As can be noted from Figs. 3-6, all the directly determined quantities (the oxide film limiting thickness, and the average oxide growth rate) and the indirectly determined quantities (the kinetic potential and number density of oxygen anions on the oxide surface) show the same type of dependence on oxygen gas pressure, reflecting the fact that the mobility of Al cations is controlled by the kinetic potential which shows a Langmuir isotherm-like dependence on the oxygen gas pressure. Our results indicate that the kinetic potential is directly related to the amount of oxygen anions formed via ionization by tunneling electrons. Since the amount of adsorbed oxygen that can be ionized by tunneling electrons is less at a lower oxygen pressure, a corresponding smaller electric potential is developed across the oxide layer. A schematic diagram of the effect of oxygen pressure described here is shown in Fig. 7. This mechanism implies that a saturated density of oxygen anions on the oxide surface would lead to the maximum kinetic potential. This is indeed the case as demonstrated in our experiments, which show that a significantly large critical oxygen gas pressure is needed such that there is sufficient adsorbed oxygen at the oxide surface to accept the tunneling electrons in order to develop the maximum kinetic potential. Beyond a critical oxygen gas pressure (~ 1 Torr) both the oxide film limiting thickness and the kinetic potential remain essentially constant, irrespective of the further increase in oxygen pressure.

5. Conclusions

We have investigated the oxidation of Al(111) for oxygen gas pressures ranging from 1×10^{-8} to 5 Torr. For all pressures, we observed an initially fast oxidation rate followed by a drastic reduction of the oxide film growth rate to reach the limiting oxide thickness. The oxide film limiting thickness is found to

increase with increasing oxygen pressure. The average oxide growth rates, kinetic potential, and the density of oxygen anions on the oxide surface are determined from the measured oxidation kinetics for the different oxygen pressures. These quantities are found to be well-described by a Langmuir isotherm dependence on the oxygen pressure owning to the Langmuir isotherm behavior of the concentration of oxygen on the surface. We show that the mobility of Al cations that governs the overall oxidation kinetics can be controlled by oxygen pressure through its influence on the kinetic potential. Our results demonstrate that the oxygen pressure can be employed instead of oxidation temperature to manipulate the self-limiting behavior of oxide film growth at low temperature.

Acknowledgement The authors gratefully acknowledge the financial support from National Science Foundation (CBET-0932814) and Basic Energy Science of Department of Energy (DE-FG02-09ER46600). Research carried out in part at the Center for Functional Nanomaterials, Brookhaven National Laboratory, which is supported by the U.S. Department of Energy, Office of Basic Energy Sciences, under Contract No. DE-AC02-98CH10886.

Reference

1 S. M. Yoon, S. H. Yang, S. H. K. Park, S. W. Jung, D. H. Cho, C. W. Byun, S. Y. Kang, C. S. Hwang, and B. G. Yu, Journal of Physics D-Applied Physics **42**, 245101 (2009).

2 K. S. Shamala, L. C. S. Murthy, and K. N. Rao, Materials Science and Engineering B-Solid State Materials for Advanced Technology **106**, 269 (2004).

3 C. M. Tanner, Y. C. Perng, C. Frewin, S. E. Saddow, and J. P. Chang, Applied Physics Letters **91**, 203510 (2007).

4 D. Tahir, H. L. Kwon, H. C. Shin, S. K. Oh, H. J. Kang, S. Heo, J. G. Chung, J. C. Lee, and S. Tougaard, Journal of Physics D-Applied Physics **43**, 255301 (2010).

5 T. Kulkarni, H. Z. Wang, S. N. Basu, and V. K. Sarin, Surface & Coatings Technology **205**, 3313 (2011).

6 H.-J. Freund and G. Pacchioni, Chemical Society Reviews **37**, 2224 (2008).

7 F. P. Fehlner, *Low-Temperature Oxidation* (John Wiley & Sons, Inc., New York, 1986).

8 I. Popova, V. Zhukov, and J. T. Yates, Jr., Phys. Rev. Lett. **89**, 276101 (2002).

9 S. K. R. S. Sankaranarayanan, E. Kaxiras, and S. Ramanathan, Phys. Rev. Lett. **102**, 095504 (2009).

10 A. Hasnaoui, O. Politano, J. M. Salazar, and G. Aral, Phys. Rev. B **73**, 035427 (2006).

11 P. C. Snijders, L. P. H. Jeurgens, and W. G. Sloof, Surf. Sci. **496**, 97 (2002).

12 L. P. H. Jeurgens, W. G. Sloof, F. D. Tichelaar, and E. J. Mittemeijer, Surf. Sci. **506**, 313 (2002).

13 L. P. H. Jeurgens, W. G. Sloof, F. D. Tichelaar, and E. J. Mittemeijer, Thin Solid Films **418**, 89 (2002).

14 N. Cabrera and N. F. Mott, Rep. Prog. Phys. **12**, 163 (1949).

15 L. P. H. Jeurgens, W. G. Sloof, F. D. Tichelaar, and E. J. Mittemeijer, J. Appl. Phys. **92**, 1649 (2002).

16 N. Cai, G. W. Zhou, K. Müller, and D. E. Starr, Phys. Rev. Lett. **107**, 035502 (2011).

17 A. T. Fromhold, Jr. and E. L. Cook, Phys. Rev. B **163**, 650 (1967).

18 F. Reichel, L. P. H. Jeurgens, and E. J. Mittemeijer, Acta Materialia **56**, 2897 (2008).

19 C. D. Wagner, L. E. Davis, M. V. Zeller, J. A. Taylor, R. H. Raymond, and L. H. Gale, Surf. Interface Anal. **3**, 211 (1981).

20 L. P. H. Jeurgens, W. G. Sloof, F. D. Tichelaar, and E. J. Mittemeijer, Phys. Rev. B. **62**, 4707 (2000).

21 H. Graupner, L. Hammer, K. Heinz, and D. M. Zehner, Surf. Sci. **380**, 335 (1997).

22 F. L. Battye, J. G. Jenkin, J. Liesegang, and R. C. G. Leckey, Phys. Rev. B **9**, 2887 (1974).

23 G. Kresse, M. Schmid, E. Napetschnig, M. Shishkin, L. Kohler, and P. Varga, Science **308**, 1440 (2005).

24 K. Christmann, *Introduction to Surface Physical Chemistry* (Springer, New York, 1991).

Figure Caption:

Fig. 1:

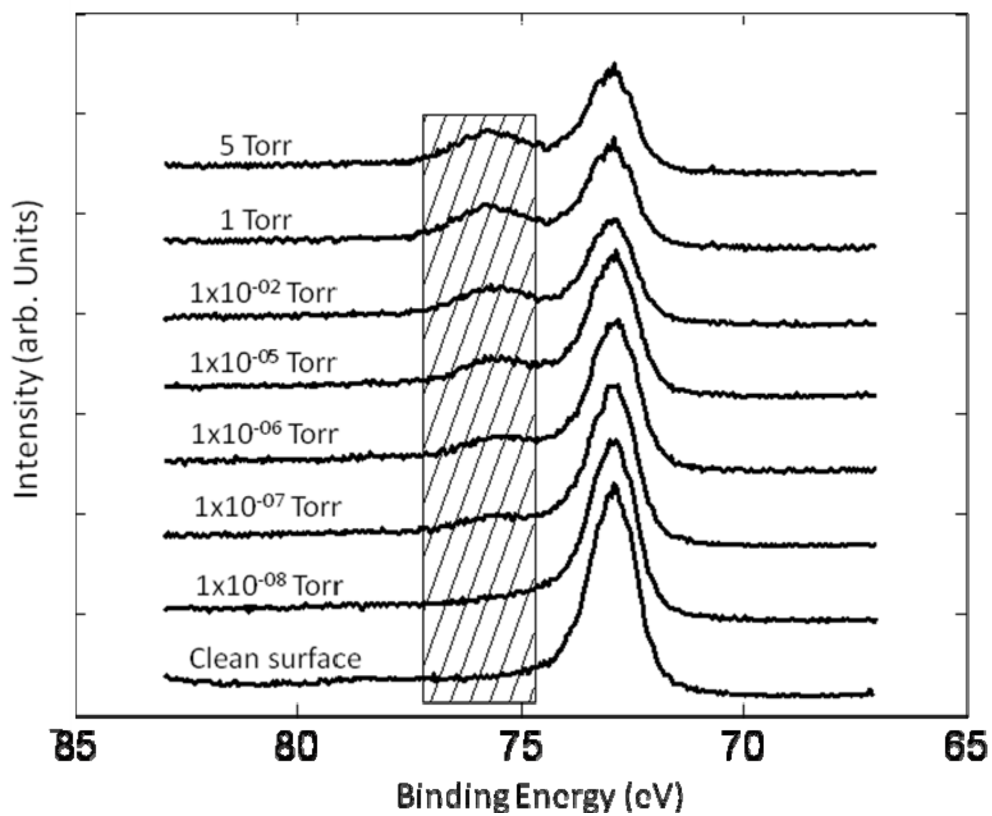

Fig. 1: Photoemission spectra of the Al 2p core level region for the freshly cleaned Al(111) surface and after extended exposures to oxygen gas at the indicated pressures.

Figure 2:

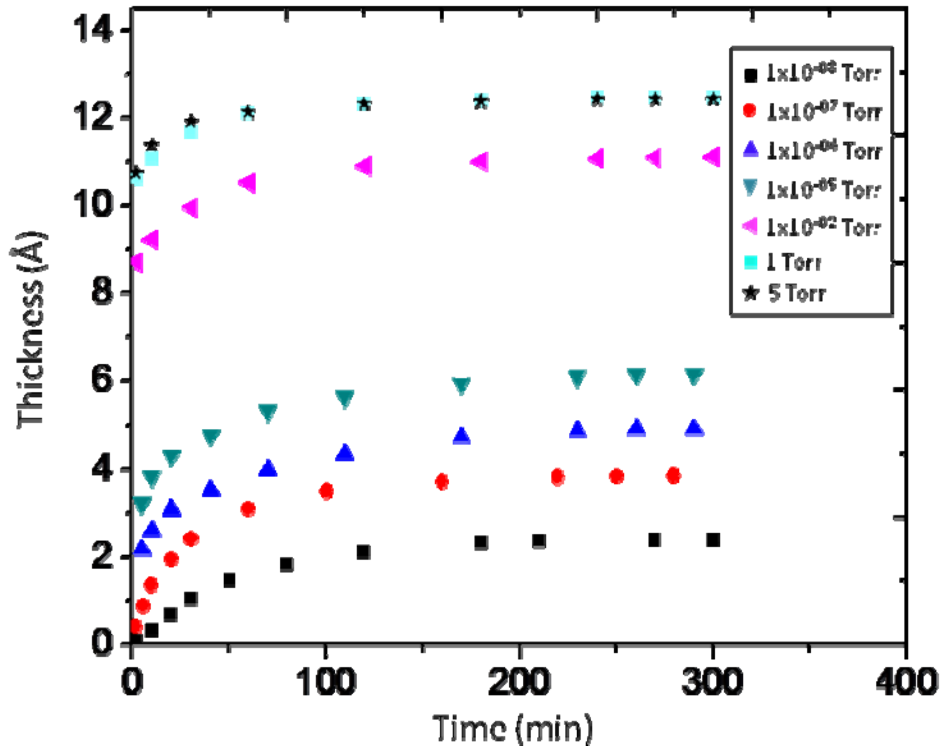

Fig. 2: The oxide thickness as a function of the oxidation time for different oxygen pressures. All spectra display an initially fast growth followed by a significant reduction in growth rate. The limiting oxide thickness increases with increasing oxygen gas pressure.

Fig. 3:

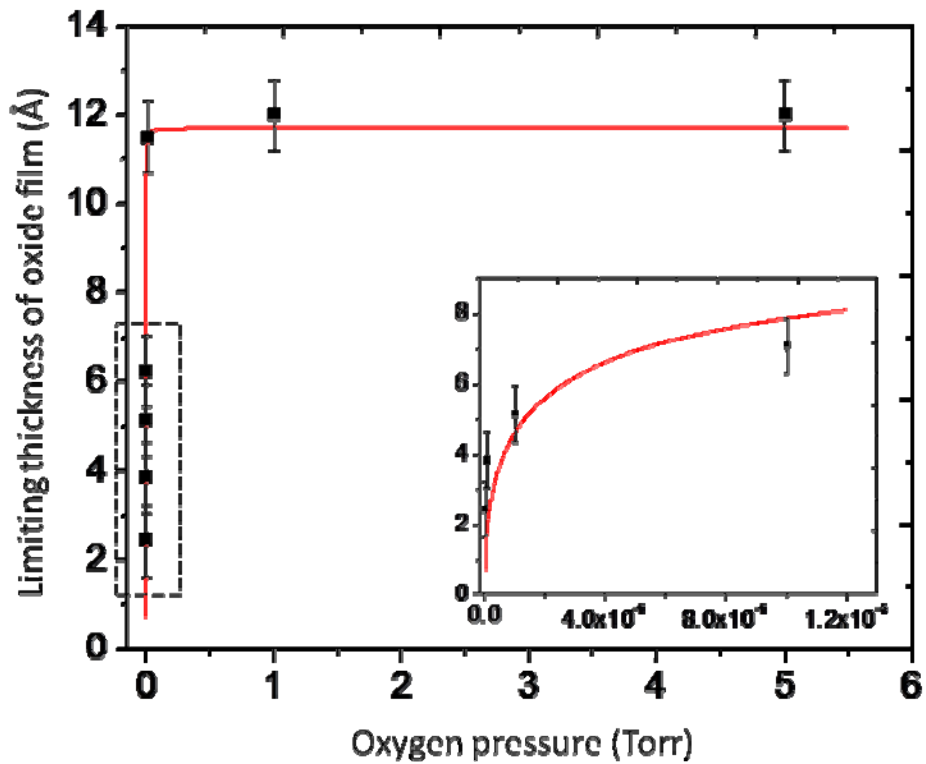

Fig. 3: The limiting thickness of the oxide films as a function of oxygen gas pressure. The limiting thickness increases with increasing oxygen gas pressure. The inset shows a zoomed-in view of the low oxygen pressure regime indicated by the dashed box.

Fig. 4:

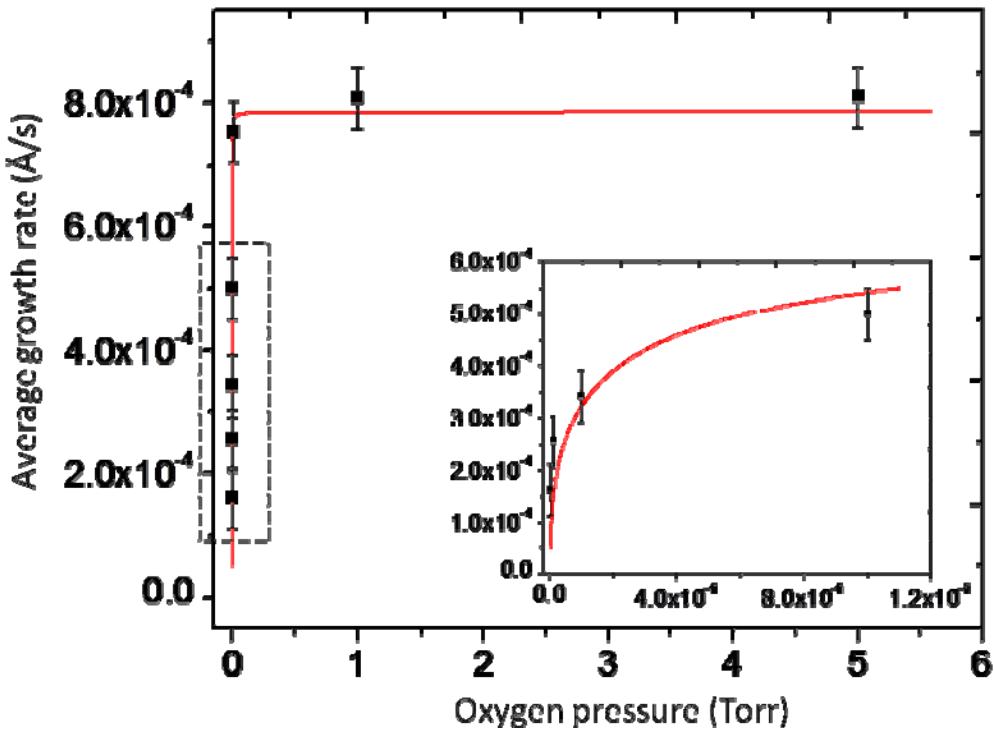

Fig. 4: Average oxide film growth rate as a function of the oxygen pressure for the oxidation of Al(111). The effective limiting oxide-film thickness is defined by the value given when the growth rate becomes less than 10^{-5} Å/s. The solid line corresponds to a fit to equation 4. The inset shows a zoomed-in view of the low oxygen pressure indicated by the dashed box.

Fig. 5:

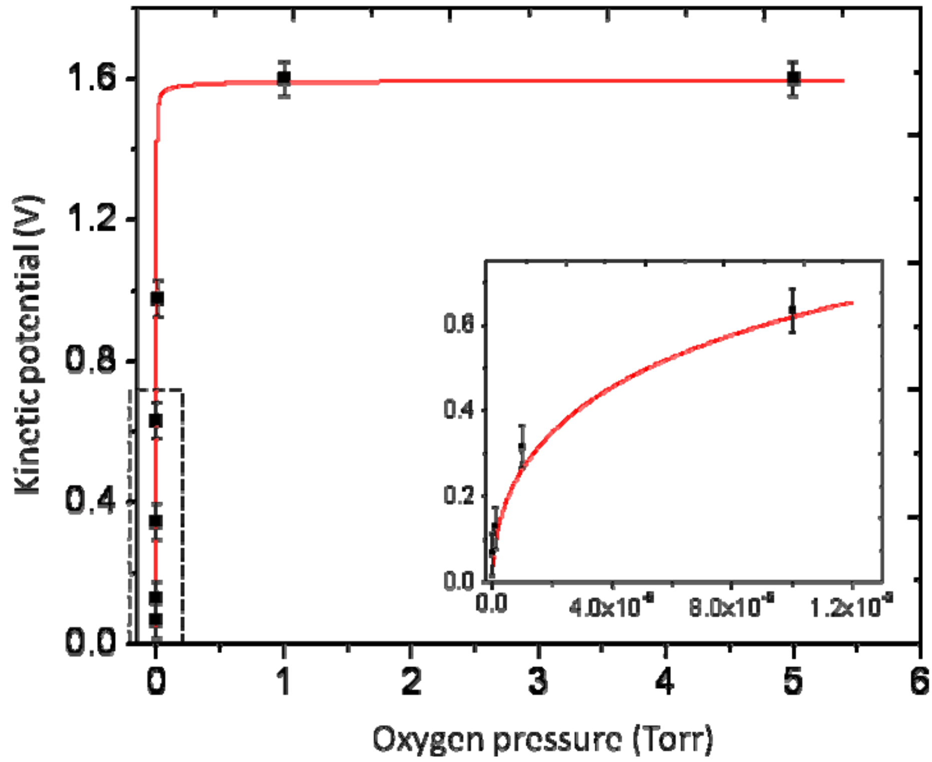

Fig. 5: Kinetic potential as a function of oxygen gas pressure. The kinetic potential increases with increasing oxygen gas pressure and leads to a pressure dependent growth behavior. The solid line is a fit to equation 3. The inset is a zoomed-in view from the region of the low oxygen pressure oxidation indicated by the dashed box.

Fig. 6

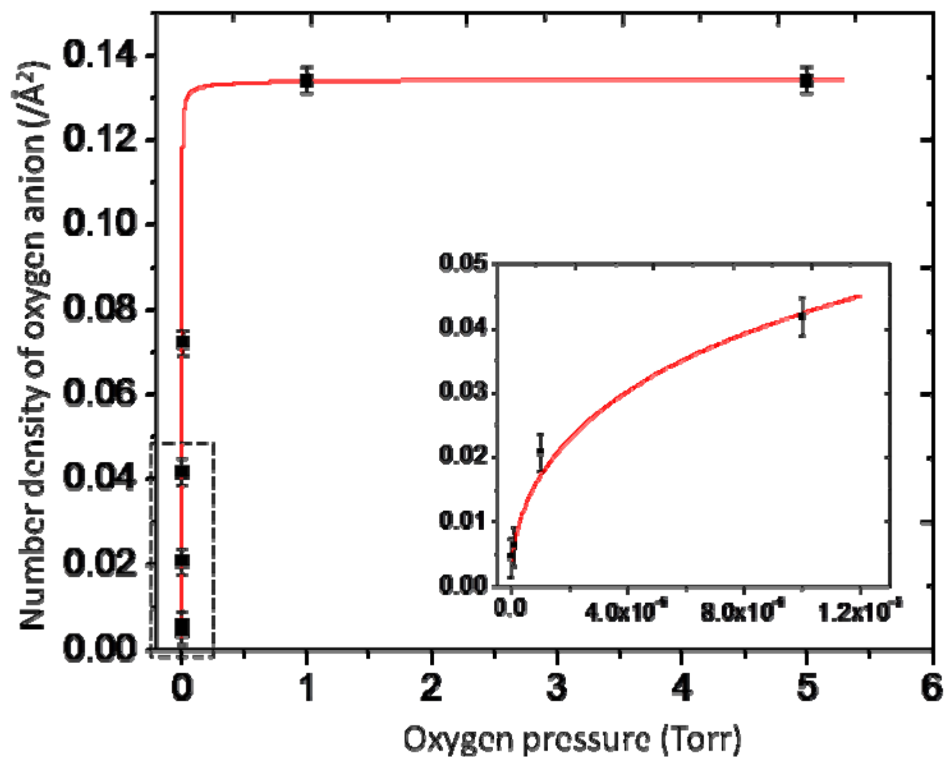

Fig. 6: The number density of chemisorbed oxygen anions on the oxide surface as a function of oxygen gas pressure. Increasing the oxygen gas pressure causes the number density of oxygen anions on the surface to increase. The solid line is a fit to the Langmuir isotherm for dissociative oxygen adsorption. The inset is a zoomed-in view of the low oxygen pressure oxidation region indicated by the dashed box.

Fig. 7

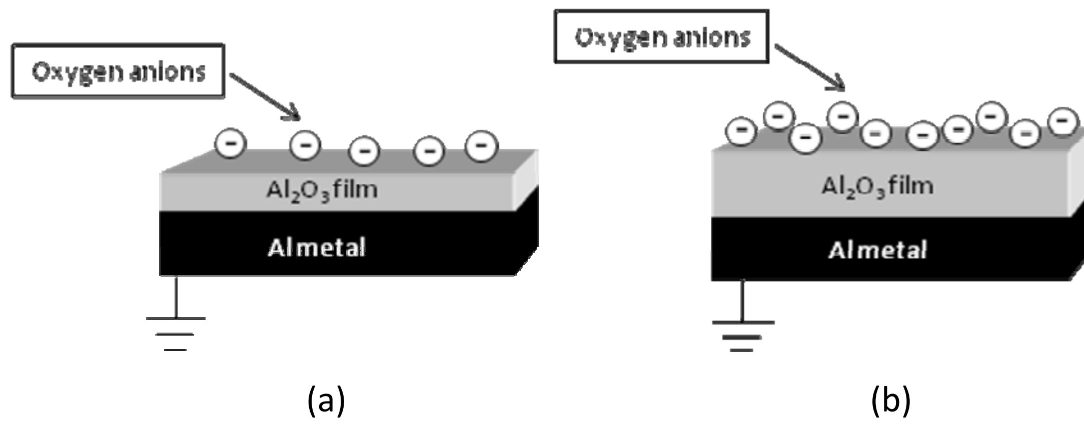

Fig. 7: Schematic model for the effect of oxygen pressure on the kinetic potential for enhancing the diffusion of Al cations through the oxide film, the rate limiting step of the Al oxidation process, at (a) low oxygen pressure, and (b) higher oxygen pressure.